HYSTERESIS, CREEP, AND VIBRATION COMPENSATION FOR PIEZOACTUATORS: FEEDBACK AND FEEDFORWARD CONTROL [1]

Kam K. Leang [2] Santosh Devasia [3]

Department of Mechanical Engineering
University of Washington
Box 352600, Seattle, Washington 98195-2600

Abstract: We present an integrated two-step approach, which combines feedback and feedforward control, to compensate for the effects of hysteresis, creep, and vibration in piezoactuators. In this approach, the control of hysteresis and creep is decoupled from the control of vibrational dynamics. First, high-gain feedback control is used to minimize positioning error caused by hysteresis and creep. Second, an inversion-based feedforward approach, which can achieve exact tracking for general output trajectories, is used to compensate for error due to vibration at high scan rates. The feedforward approach is applicable to minimum (collocated sensor and actuator) and nonminimum phase (noncollocated sensor and actuator) positioning systems. The decoupling of hysteresis and creep control from vibration control simplifies the inversion-based approach, and the use of feedback provides robustness. We show significant improvement in positioning precision and scanning rate, and illustrate our results with an experimental piezoactuator scanner that is used in Atomic Force Microscope (AFM) applications.

Keywords: Hysteresis, Creep, Vibration, High-gain Feedback, Feedforward Control.

1. INTRODUCTION

In this article, we present a two-step approach to compensate for hysteresis, creep, and vibration effects in piezoactuators. The proposed approach decouples the control of hysteresis and creep from the control of vibrational dynamics. First, high-gain feedback is used to reduce positioning error caused by hysteresis and creep. Second, a recently developed inversion-based feedforward approach (Bayo, 1987; Dewey *et al.*, 1998) is used to exploit the known dynamics of the piezoactuator for finding feedforward inputs for vibration compensation at high scan rates. The integrated approach yields high-precision piezo-positioning over long ranges (through hysteresis compensation), extended periods of time (through creep compensation), and at high scan rates (through vibration compensation). Such precise positioning of the piezoactuator is important to the development of high performance mechatronic tools for machining (Okazaki, 1990), bioengineering applications (Stilson *et al.*, 2001), and nanotechnology (Quate, 1997).

Piezoactuators are capable of ultra-high resolution positioning and have been exploited in a wide variety of precision mechatronic systems; for example, in auto focus systems, laser tuning, disk drive applications, micropumps, and microlithography. However, their performance is still limited by three major factors: (1) hysteresis, (2) creep,

[1] Acknowledgment Grant NAG 2-1450 and Grant NSF-CMS 0196214
[2] Graduate student; E-mail: kleang@u.washington.edu
[3] Associate Professor; Tel: 206.685.3401; E-mail: devasia@u.washington.edu

and (3) induced structural vibration. First, the nonlinear relationship between the applied voltage and the displacement of a piezoactuator, known as hysteresis, contributes to positioning error (Cao and Evans, 1993). Hysteresis is more pronounced over long range operations and can easily be avoided by operating in the linear range, i.e., over short displacements. However, by avoiding hysteresis, a designer sacrifices a piezoactuator's ability to displace over long ranges with sub-angstrom level precision. Second, piezoactuators tend to creep over extended periods of time (i.e., during slow scan rates), a behavior that also contributes to loss in positioning precision (Fett and Thun, 1998). Positioning offset from the center of a piezoactuator's displacement range amplifies the effect of creep, therefore making absolute positioning and calibration difficult. One method to avoid creep is to operate fast enough that the effect becomes negligible, but this method restricts piezoactuators from slow and static operations. The combined effects of hysteresis and creep can amount to as much as 50 percent error in calibration, such as in scanning probe microscopy (SPM) applications (Barrett and Quate, 1991). Third, scanning at high rates relative to the first vibrational frequency can induce structural vibration, causing significant positioning error. Typically, scanning rates are restricted to less than 1/10th to 1/100th of the first vibrational frequency, thus limiting the scanning rate of such systems. Faster scanning can be achieved using stiffer piezoactuators with high resonance frequencies, but this reduces the effective displacement range of the positioner. The compound effects of hysteresis, creep, and vibration can significantly limit the performance of piezoactuators. For example, in ultra-high precision machining, hysteresis and creep effects can limit surface form accuracy (Okazaki, 1990). In nanotechnology, distortion in SPM-based imaging caused by hysteresis, creep, and vibration can make accurate surface characterization difficult and slow (Barrett and Quate, 1991). Therefore, precision control of all three effects is critical to future development of high performance piezo-based mechatronic positioning systems.

A variety of approaches have been investigated to improve the positioning performance of piezoelectric actuators. Feedback control schemes such as proportional-integral-derivative (PID) (Barrett and Quate, 1991), state-feedback (Okazaki, 1990), and H_∞ control (Korson and Helmicki, 1995) have all demonstrated substantial improvements in positioning under the influences of hysteresis and creep. The advantages of feedback control includes ease of implementation, and robustness to modeling uncertainties and parameter variation (Franklin *et al.*, 1994). However, there is a limitation to the achievable transient response when using feedback control because turnaround transients cause excessive oscillations at high scan rates (Barrett and Quate, 1991). By using charge control (rather than voltage control), the effects of hysteresis and creep are significantly reduced, but at the cost of reducing the effective displacement range of the actuator (Kaizuka and Siu, 1988). Another example of hysteresis compensation is feedforward control, in which inputs are computed using the classic Preisach hysteresis model (Schafer and Janocha, 1995). A related approach, known as phase control, in which the hysteresis nonlinearity is handled as a phase lag, has been developed (Cruz-Hernandez and Hayward, 2001). The efficacy of the feedforward Preisach model-based approach is combined with a regular PID control scheme to further improve tracking performance (Majima *et al.*, 2001; Ge and Jouaneh, 1996). High scan rate tracking is demonstrated, but only for a sinusoidal reference trajectory (0.1-20 Hz) (Ge and Jouaneh, 1996). Recently, an inversion-based feedforward approach was presented to compensate for all three adverse effects for both minimum (collocated sensor and actuator) and non-minimum phase (noncollocated sensor and actuator) positioning systems; however, this approach requires extensive modeling and is sensitive to modeling uncertainty (Croft *et al.*, 2001).

We present an integrated feedback and feedforward approach to account for all three effects, which provides robustness and achievable tracking for general output trajectories. The approach is a two-step process, in which hysteresis and creep control are decoupled from vibration control. Specifically, high-gain feedback control is used for hysteresis and creep compensation, and a model-based inverse feedforward technique (which has been successfully applied to other flexible structures (Dewey *et al.*, 1998)) is used for vibration compensation. The feedback controller provides robustness for the inversion-based approach, (i.e., robust to modeling uncertainties or parameter variation in the system), and the inversion-based feedforward approach achieves exact tracking for general output trajectories (Bayo, 1987). Figure 1 is a schematic of the control scheme to be considered herein. This integrated approach yields precision piezo-positioning over long ranges, extended periods of time, and at high scan rates. We show a significant improvement in positioning precision and scanning rate, and demonstrate our results with an experimental piezoactuator system.

The remainder of this article is organized as follows. We describe the reduction of hysteresis and creep using high-gain feedback control in Section 2. In addition, we describe the design of a notch filter for increasing the gain margin needed to

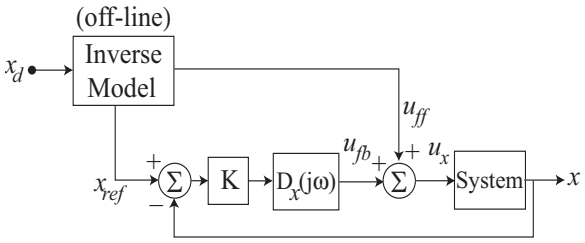

Fig. 1. Block diagram of control system where u_{fb} and u_{ff} are the feedback and feedforward inputs, respectively; u_x is the input to the system; K is the proportional gain; $D_x(j\omega)$ is the notch filter for improving gain margin; x_d is the desired output trajectory; x_{ref} is the reference trajectory to the feedback system; x is the actual system output.

enable the use of high-gain feedback. In Section 3, we present the model-based inversion feedforward technique. The feedforward input, used to compensate for induced structural vibration at high scan rates, is computed for the feedback linearized system. A discussion of the experimental results is presented in Section 4, and concluding remarks follow in Section 5.

2. HYSTERESIS AND CREEP COMPENSATION: HIGH-GAIN FEEDBACK CONTROL

2.1 *System description and modeling*

The experimental piezoactuator system studied in this article is the scanner device (lead-zirconate-titanate (PZT)) used in the Burleigh Metris 2000NC Atomic Force Microscope (AFM). The function of the piezoactuator is to position a sample relative to a cantilever and probe tip along the x-, y-, and z-axis as shown in Figure 2. Scanning is performed parallel to the sample surface (along the x- and y-axis). As the sample is scanned relative to the probe tip, surface contours deflect the cantilever beam perpendicular (z-axis) to the sample surface. The deflection of the beam is measured by an optical sensor and a z-axis feedback controller is used to maintain appropriate tip-to-sample separation for *contact* and *non-contact* mode operations. The output of the optical sensor (height in z-direction) is used to construct an image of the topology of the sample surface (Binnig and Quate, 1986). In our system, hysteresis, creep, and vibration compensation is considered for both the x- and y-axis; however, we present the details of our analysis and design only for scanning along the x-direction. Scanning along the y-direction is similar, and its presentation is omitted for brevity.

The vibrational dynamics of the piezoactuator in the x-direction ($G_x(j\omega)$) was measured with

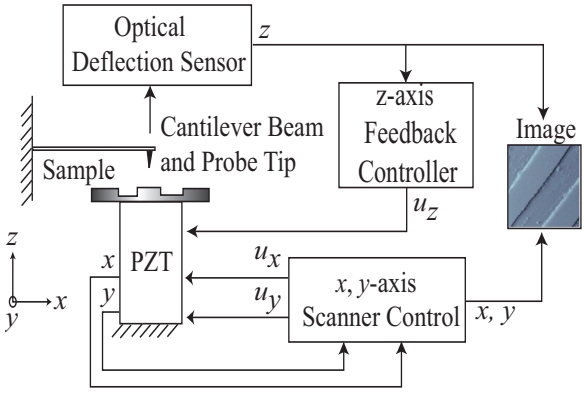

Fig. 2. Schematic of Atomic Force Microscope (AFM).

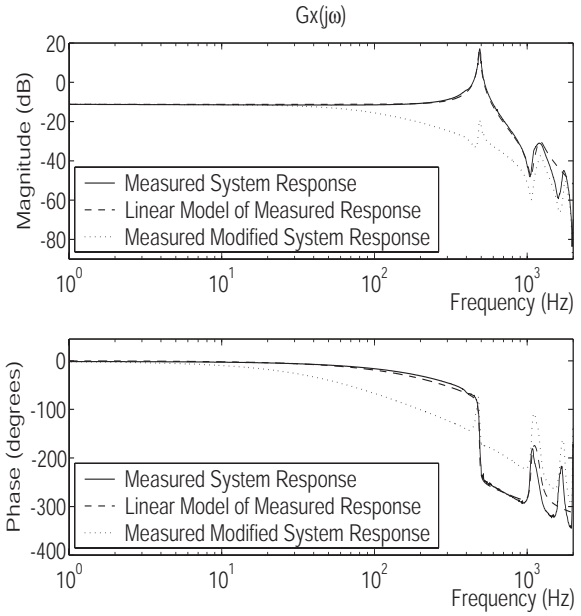

Fig. 3. Frequency response of the experimental piezoactuator system over small displacements: measured (solid line), linear model (dashed line), and piezoactuator cascaded with the notch filter (dotted line). The linear model is a good fit of the measured response up to 1.3 kHz.

a dynamic signal analyzer (DSA) (Stanford Research Systems SR785) over small displacement ranges where hysteresis is negligible (i.e., 10% of the maximum displacement range). A command voltage u_x (*Volts*) from the DSA was applied to the x-direction of the piezoactuator. The resulting displacement in the x-direction was measured (in *Volts*) by an optical sensor and fed back to the DSA to construct the frequency response curve (solid line in Figure 3). A linear model (dashed line in Figure 3), represented as a transfer function in the frequency domain, relating the input voltage to the piezoactuator u_x and the output displacement x, was fitted to the measured response. The model was found to be

$$G_x(j\omega) = (2\pi)^4 k_x \frac{\prod_{m=1}^{2}(j\omega - 2\pi z_m)}{\prod_{n=1}^{6}(j\omega - 2\pi p_n)} := \frac{n_x(j\omega)}{d_x(j\omega)}, \quad (1)$$

where $k_x = 4.11 \times 10^{10}$, and the zeros ($z_m$, for $m = 1, \cdots, 2$) and poles (p_n, for $n = 1, \cdots, 6$) of the system are presented in Table 1. The linear model is a good fit up to approximately 1.3 kHz, as indicated in Figure 3 by the deviation of the model from the measured response near the frequency 1.3 kHz.

The measured frequency response reveals a sharp resonant peak at 486 Hz, which limits scanning to very low frequencies (typically 10-100 times lower than the first resonance frequency). The experimental piezoactuator scanner used in the AFM system typically operates in open-loop mode less than 5 Hz to avoid vibration effects.

In the next section, we use high-gain feedback control for hysteresis and creep compensation. After hysteresis and creep effects have been minimized, we use the linear model $G_x(j\omega)$ in an inversion-based approach to find feedforward inputs to compensate for induced structural vibrations at high scan rates.

2.2 *Improving gain margin*

High-gain feedback control can be used to reduce hysteresis and creep effects; however, it cannot be used if the system has relatively low gain margin for stability. In particular for piezos, the sharp resonant peak gives rise to low gain margin. For example, the measured gain margin in our experimental system is -16.67 dB (Figure 3). In its current state, the system is stable only for very low feedback gains ($K < 0.147$). This observation motivates improvement of the gain margin by cascading a notch filter $D_x(j\omega)$ to the original system (i.e., in (Okazaki, 1990); shown in Figure 1). The transfer function (in the frequency domain) of the notch filter is given by

$$D_x(j\omega) = k_D \frac{(j\omega - 2\pi z_1)(j\omega - 2\pi z_2)}{(j\omega - 2\pi p_1)(j\omega - 2\pi p_2)} \quad (2)$$

where $k_D = 2.22$, $z_1 = -4 + 475j$ Hz, $z_2 = -4 - 475j$ Hz, $p_1 = -100$ Hz, and $p_2 = -5000$ Hz. The dotted line in Figure 3 represents the measured frequency response of the notch filter cascaded with the experimental piezoactuator. The effect of the sharp resonant peak is reduced, thereby, improving the gain margin to 31.78 dB. The maximum allowable feedback gain is 38.82, making high-gain feedback compensation of hysteresis and creep feasible.

Table 1. Zeros and poles of PZT model.

m, n	**Zeros** (z_m) $[Hz]$	**Poles** (p_n) $[Hz]$
1	-25 + 1059j	-411
2	-25 - 1059j	-5 + 486j
3	n/a	-5 - 486j
4	n/a	-70 + 1200j
5	n/a	-70 - 1200j
6	n/a	-1200

2.3 *High-gain feedback control*

A proportional feedback controller is used to compensate for hysteresis and creep, and is implemented using analog Op-Amp circuits (Figure 1). The feedback gain was chosen to be $K = 20 \leq K_{max} = 38.82$ (31.78 dB), high enough to achieve adequate hysteresis and creep compensation, yet low enough to avoid instability in the closed-loop system.

2.3.1. *Hysteresis Compensation Results* Experiments were performed to demonstrate hysteresis compensation using high-gain feedback control. The hysteresis curve in Figure 4a plots the measured displacement x versus the desired response x_d for two cases: (1) without (dashed line), and (2) with high-gain feedback compensation (solid line). The scanning frequency was 1 Hz, slow enough that dynamic effects could be neglected, yet fast enough that creep was negligible. The desired scan range is 50.00 μm (± 25.00 μm, or ± 1.25 V measured by the position sensor), a range in which hysteresis is clearly noticeable in the output displacement without compensation. Ideally, the response of the system should fall on the dotted line (linear response); however, without compensation (case (1), dashed line) there is significant positioning error due to hysteresis. The output hysteresis is defined as the displacement measured between a point on the ascending path and a corresponding point on the descending path of the hysteresis curve (Cruz-Hernandez and Hayward, 2001), see Figure 4a. The maximum output hysteresis is 6.29 μm, 12.58 percent of the total output range (50 μm). The experiment also revealed that the gain of the system (output-to-input ratio) varies with output amplitude, where the slope of the piezoactuator displacement versus applied voltage curve increases with the scanning voltage (Barrett and Quate, 1991). Hysteresis was significantly reduced with high-gain feedback control (case (2), solid line), and the measured output hysteresis with feedback compensation is 1.04 μm, a reduction of over 83 percent compared to the uncompensated case. The discrepancy in the slope between the compensated result and the linear response can be attributed to limitations of the feedback controller. Although larger feedback gains can further improve the performance, improvement is limited by the gain margin.

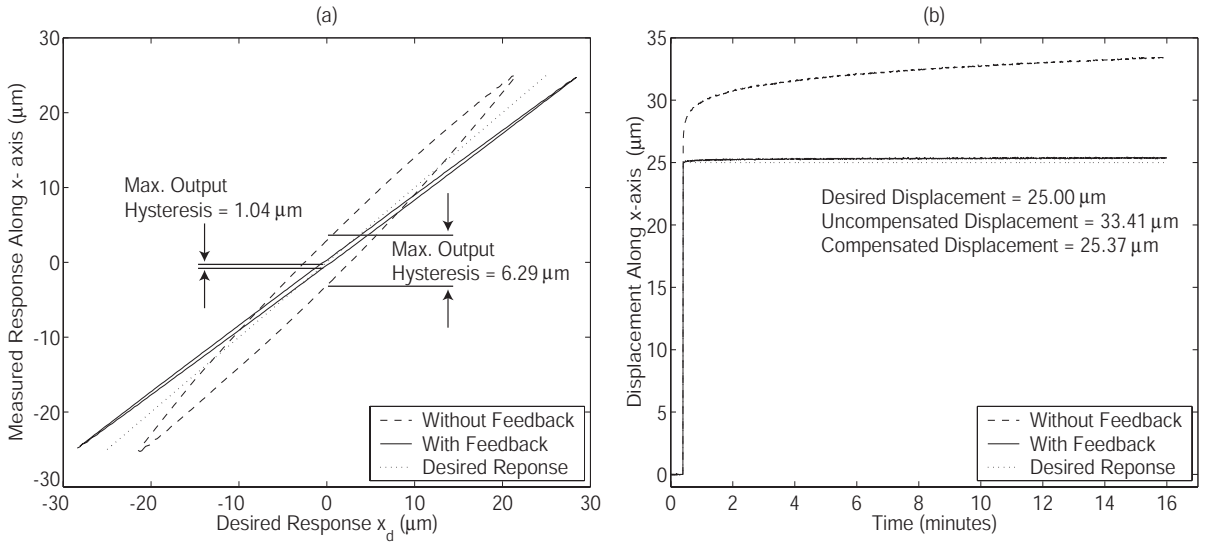

Fig. 4. Experimental results showing (a) hysteresis and (b) creep compensation using high-gain feedback. Dashed line is without compensation; solid line is with compensation; and dotted line is the desired response.

2.3.2. *Creep Compensation Results* Experiments were performed to demonstrate creep compensation using high-gain feedback control. Figure 4b shows a step response (measured over a period of 15 minutes) of the piezoactuator comparing two cases: (1) without (dashed line), and (2) with high-gain feedback compensation (solid line). The desired output displacement is 25.00 μm (dotted line). For case (1), the output displacement measured after 15 minutes was 33.41 μm, a 8.41 μm error in positioning. However, with high-gain feedback compensation (case (2), solid line) the effect of creep was minimized and the displacement measured after 15 minutes was 25.37 μm, a 0.37 μm error in positioning, and a 95 percent reduction in positioning error using high-gain feedback compensation.

High-gain feedback control improves the closed-loop response and significantly reduces the effects of hysteresis and creep by over 83 and 95 percent, respectively. In addition, the feedback controller is robust to modeling uncertainty and parameter variation, for example by minimizing the effect of amplitude dependent gain (output-to-input ratio) in the experimental piezoactuator. Next, inversion-based feedforward control is combined with high-gain feedback control for high-precision positioning at high scan rates.

3. VIBRATION COMPENSATION: INVERSION-BASED FEEDFORWARD CONTROL

Vibration compensation is achieved by exploiting the known dynamics of the piezoactuator for finding feedforward inputs to minimize tracking error at high scan rates. The linear model of the x-direction vibrational dynamics ($G_x(j\omega) = n_x(j\omega)/d_x(j\omega)$, Equation 1) is inverted to find the feedforward input u_{ff}. A technique has been developed for linear time-invariant nonminimum phase systems (Bayo, 1987). However, the feedforward input generated by this approach can lead to input saturation because of the excessively large input required for exact tracking of certain trajectories. Therefore, we are motivated to consider the optimal stable inversion approach (Dewey *et al.*, 1998), which poses the optimal inversion trajectory redesign problem as the minimization of the following objective cost function:

$$J(u) = \int_{-\infty}^{+\infty} \{u^*(j\omega)R(j\omega)u(j\omega) + [x(j\omega) - x_d(j\omega)]^* \times Q(j\omega)[x(j\omega) - x_d(j\omega)]\}d\omega, \quad (3)$$

where each term is expressed in the frequency domain. The superscript * denotes complex conjugate transpose, and x_d is the desired scan path.

The terms $R(j\omega)$ and $Q(j\omega)$ in our objective cost function represent frequency dependant real-valued weightings on the input u and tracking error $x - x_d$, respectively. Both values should not be simultaneously zero at any frequency. We point out two extreme cases for the choice of R and Q. First, if the weight on the tracking error is zero (i.e., $Q = 0$) and R nonzero, then not tracking the desired trajectory x_d would be the best approach. In the second case, if $R = 0$ and Q nonzero, the best strategy is to track the desired scan path exactly, i.e., $x = x_d$. Note that in the second case, the input from the optimal inverse is the input from the exact-inverse, which allows the

system to precisely track the desired scan path x_d. For a discussion of trade-offs and various design approaches using this technique see (Brinkerhoff and Devasia, 1999).

By minimizing the objective cost function equation (3), the optimal input for the x-direction $u_{x,opt}$ is:

$$u_{x,opt}(j\omega) = \left[\frac{G^*(j\omega)Q(j\omega)}{R(j\omega) + G^*(j\omega)Q(j\omega)G(j\omega)}\right] \times x_d(j\omega). \quad (4)$$

The optimal input $u_{x,opt}$ and optimal desired trajectory x_{opt} can be found such that vibrations and actuator saturation are minimized.

A block diagram of the combined feedback and feedforward controllers is shown in Figure 1. Note that the optimal inversion is computed off-line. The optimal input ($u_{x,opt} = u_{ff}$) generated from the off-line inversion technique is added to the on-line feedback input u_{fb}, and the sum ($u_x = u_{ff} + u_{fb}$) is applied to the system. The redesigned optimal trajectory x_{opt} from the off-line inversion approach is used as the reference trajectory x_{ref} to the feedback system (i.e., $x_{ref} = x_{opt}$).

3.1 *Vibration Compensation Results*

Experiments were performed to demonstrate vibration compensation using inversion-based feedforward control, and results for scanning at 30 Hz are shown in Figure 5. At this frequency, the effect of vibrational dynamics on the piezoactuator without feedforward compensation is significant, and this can lead to distortion in AFM imaging (Barrett and Quate, 1991). In the experiment, the desired scan range is 50.00 μm ($\pm$25.00 μm). Two cases were investigated: (1) without (dashed line) and (2) with inverse compensation (solid line), as illustrated in Figure 5. The feedforward input ($u_{ff} = u_{x,opt}$) was computed for the feedback linearized system (Equation (1)) using the optimal inversion-based approach. The weighting values for the optimal inversion are: $Q = 1$ and $R = 0$ for $\omega \leq 650$ Hz, and $Q = 0$ and $R = 1$ for $\omega > 650$ Hz. The criteria for choosing 650 Hz as the cutoff frequency was based on the bandwidth of $G_x(j\omega)$ (Figure 3). For case (1), the optimal desired trajectory x_{opt} generated from the optimal inverse was used as a reference trajectory x_{ref} to the feedback system (i.e., $x_{ref} = x_{opt}$). For case (2), the inverse feedforward input $u_{ff} = u_{x,opt}$ was added to the feedback input u_{fb}, and the sum ($u_x = u_{ff} + u_{fb}$) was applied to the system (see Figure 1). Without inverse compensation (case (1), dashed line) the maximum tracking error $x - x_d$ is 4.03 μm, 8.06 percent of the total output range (50 μm). In contrast, inverse compensation

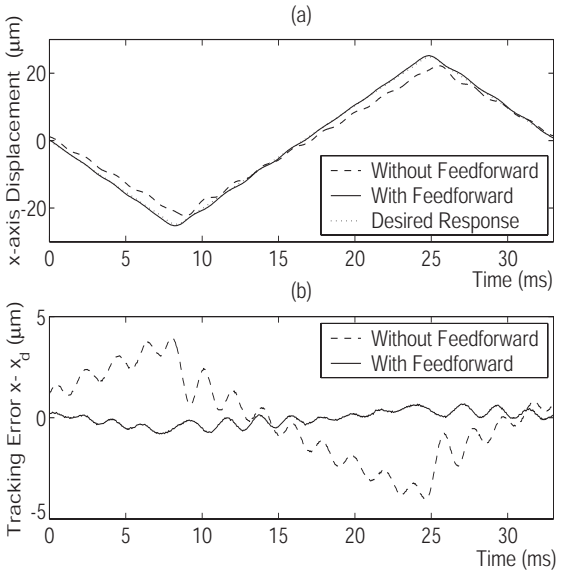

Fig. 5. Experimental results. (a) Scan-path tracking at 30 Hz showing desired response (dotted line), response without (dashed line), and with inverse compensation (solid line). (b) Tracking error without (dashed line) and with inverse compensation (solid line).

reduced the maximum tracking error to 0.80 μm, a reduction of 80 percent compared to the uncompensated case, as illustrated in Figure 5b. Inverse compensation minimized vibration and corrected for phase lag, substantially improving tracking performance at high scan rates.

4. DISCUSSION

The proposed integrated two-step approach, which combines feedback (for hysteresis and creep compensation) and inversion-based feedforward control (for vibration compensation), significantly minimizes the effects of hysteresis, creep, and vibration in piezoactuators. Experimental results shown in Figures 4 and 5 demonstrate significant improvement in positioning precision and scanning rate.

By decoupling the control of nonlinear hysteresis and creep from the control of vibrational dynamics, each effect is handled independently. Figure 4 illustrates that high-gain feedback control effectively minimizes errors caused by hysteresis and creep (by over 83 and 95 percent, respectively). In addition, feedback control minimizes the effect of parameter variation, such as the amplitude dependent gain (output-to-input ratio) of the experimental piezoactuator. For slow enough scan rates, feedback control can improve positioning precision, such as absolute positioning and calibration of piezo-based systems, as well as minimize distortion in AFM imaging due to hysteresis and creep (Croft *et al.*, 2001).

However, at high scan rates (30 Hz in the experiment), feedback control provides limited compensation for errors due to induced structural vibration and phase lag (Figure 5a (dashed line)). In the experiment, tracking error was 8.09 percent of the total output range without inverse compensation. The error was reduced by 80 percent (Figure 5) using the optimal inversion-based approach. By decoupling the control of hysteresis and creep from vibrational dynamics, the inversion-based approach is simplified because the effects of hysteresis and creep do not have to be modeled in the feedforward input; modeling hysteresis and creep can be a tedious task (Croft *et al.*, 2001). Also, feedback control provides robustness to the inversion-based approach, helping to account for modeling uncertainties that are poorly represented by the model, for example the amplitude dependent gain of the system. For nonminimum phase piezo-based positioning systems, the selected inversion-based approach can achieve exact output tracking of general trajectories.

The significant reduction in tracking errors and increase in scanning rate using this integrated approach will greatly improve positioning precision of piezo-based mechatronic systems.

5. CONCLUSION

The proposed integrated high-gain feedback and inversion-based feedforward control substantially minimizes the error caused by hysteresis, creep, and vibration. We demonstrate a significant performance increase for an experimental piezoactuator system and offer a solution for high-speed ultra-precision positioning over long ranges, extended periods of time, and at high scan rates. The two-step approach decouples the control of hysteresis and creep from vibrational dynamics, thereby simplifying the inversion-based approach. The feedback controller provides robustness, and the inversion-based feedforward approach can achieve exact output tracking for minimum and nonminimum phase positioning systems. Future work will focus on methods of improving the inversion-based approach using iterative learning techniques for faster scanning.

6. REFERENCES

Barrett, R.C. and C.F. Quate (1991). Optical scan-correction system applied to atomic force microscopy. *Rev. Sci. Instrum.* **62**(6), 1393–1399.

Bayo, E. (1987). A finite-element approach to control the end-point motion of a single-link flexible robot. *J. Robotic Syst.* **4**, 63–75.

Binnig, G. and C.F. Quate (1986). Atomic force microscope. *Phys. Rev. Lett.* **56**(9), 930–933.

Brinkerhoff, R. and S. Devasia (1999). Output tracking for actuator deficient/redundant systems: multiple piezoactuator example. *AIAA J. Guid. Contr., and Dynamics* **23**(2), 370–373.

Cao, H. and A.G. Evans (1993). Nonlinear deformation of ferroelectric ceramics. *J. Amer. Ceram. Soc.* **76**, 890–896.

Croft, D., G. Shed and S. Devasia (2001). Creep, hysteresis, and vibration compensation for piezoactuators: atomic force microscopy application. *ASME J. Dyn. Syst., Meas., and Control* **123**, 35–43.

Cruz-Hernandez, J.M. and V. Hayward (2001). Phase control approach to hysteresis reduction. *IEEE Trans. Contr. Syst. Tech.* **9**(1), 17–26.

Dewey, J.S., K. Leang and S. Devasia (1998). Experimental and theoretical results in output-trajectory redesign for flexible structures. *ASME J. Dyn. Syst., Meas., and Control* **120**, 456–461.

Fett, T. and G. Thun (1998). Determination of room-temperature tensile creep of PZT. *J. Mater. Sci. Lett.* **17**(22), 1929–1931.

Franklin, G. F., J. D. Powell and A. Emami-Naeini (1994). *Feedback control of dynamic systems, 3rd Edition*. Addison-Wesley. New York.

Ge, P. and M. Jouaneh (1996). Tracking control of a piezoceramic actuator. *IEEE Trans. Contr. Syst. Tech.* **4**(3), 209–216.

Kaizuka, H. and B. Siu (1988). A simple way to reduce hysteresis and creep when using piezoelectric actuators. *Jap. J. Appl. Physics* **27**(5), 773–776.

Korson, S. and A.J. Helmicki (1995). An H_∞ based controller for a gas turbine clearance control system. *IEEE Conf. Contr. Applicat.* pp. 1154–1159.

Majima, S., K. Kodama and T. Hasegawa (2001). Modeling of shape memory alloy actuator and tracking control system with the model. *IEEE Trans. Contr. Syst. Tech.* **9**(1), 54–59.

Okazaki, Y. (1990). A micro-positioning tool post using a piezoelectric actuator for diamond turning machines. *Precision Engineering* **12**(3), 151–156.

Quate, C.F. (1997). Scanning probes as a lithography tool for nanostructures. *Surface Science* **386**, 259–264.

Schafer, J. and H. Janocha (1995). Compensation of hysteresis in solid-state actuators. *Sensors and Actuators A* **49**, 97–102.

Stilson, S., A. McClellan and S. Devasia (2001). High-speed solution switching using piezo-based micro-positioning stages. *Proc. Amer. Contr. Conf.* **3**, 2238–2243.